This full text paper was peer-reviewed at the direction of IEEE Instrumentation and Measurement Society prior to the acceptance and publication.

Lake water level estimated by a purely radiometric measurement: an experiment with the SLSTR radiometer onboard Sentinel-3 satellites

Andrea Scozzari
Institute of Information Science and Technologies
National Research Council of Italy
Pisa, Italy
a.scozzari@isti.cnr.it

Stefano Vignudelli
Institute of Biophysics
National Research Council of Italy
Pisa, Italy
vignudelli@pi.ibf.cnr.it

Abdelazim Negm
Faculty of Engineering
Zagazig University
Zagazig, Egypt
amnegm@zu.edu.eg

***Abstract*— This work describes a preliminary study on the possible usage of the imaging radiometer SLSTR (Sea and Land Surface Temperature Radiometer) onboard the Sentinel-3 satellites for estimating quantitative parameters (extent and/or level) of inland water bodies. Various works in the literature propose a combination of optical imagery and radar altimetry to estimate water storage variations in inland water targets. This work wants to exploit the simultaneous acquisition offered by SRAL (Synthetic aperture Radar ALtimeter) and SLSTR instruments hosted by the Sentinel-3A/B platform. We present a practical case study, demonstrating how a strongly reduced subset of radiometric measurements can be enough representative of the status of the natural system under observation. In our approach, a subset of the collected radiance maps is extracted, based on the selection of the most variable pixels. Thus, a time series of average spectral radiances is built upon the reduced set of SLSTR data, and compared with satellite radar altimetry measurements. Preliminary results show a promising relationship between the timeseries generated by the two independent instruments, in terms of both general trend and seasonal dependence. Finally, by using the approximation proposed in this paper, a very light computational process can infer an estimation of water storage, when the natural system is fully identified on the basis of ground-truth data.**

Keywords—environmental measurements, radiometry, water level, satellite remote sensing

I. INTRODUCTION

The measurement of electromagnetic quantities and the processing of the data generated by imaging sensors constitute the technological foundation for a vast quantity of environmental measurement applications, particularly since when the technology is offering relatively low-cost imaging sensors, with a sufficient radiometric performance for many purposes.

In the time of Internet of Things and of distributed processing by cloud computing, the paradigm of inexpensive, light and distributed sensing systems generating a big quantity of data has an unquestionable appeal. In fact, environmental measurements in recent times took advantage from many common devices, e.g. microbolometer arrays for thermographic imaging [1, 2, 3], CMOS cameras for optical sensing in the visible and near-infrared domains [4, 5], and even smartphone cameras used as communication and sensing devices [6, 7, 8, 9].

Today, mobile networking enables also the usage of smart portable devices for citizen/crowdsourced observations, which have been proposed as a valid resource for several environmental applications. As an example, in the hydrological context, crowdsourced information (essentially, pictures) gathered by mobile phones is proposed for the monitoring of critical sites and to provide useful data for the improvement of models [10]. In addition, light multi/hyper-spectral cameras and thermal infrared radiometers are often proposed to be mounted on drones for environmental monitoring [11].

On the other hand, technologies enabling high measurement performance, especially in terms of repeatability, are still essential for quantitative assessments in the observation of the environment. This aspect applies certainly to the context of radiometric measurements. In particular, remotely sensed images from satellite-borne imaging radiometers still play a relevant role under two essential conditions: i) be complementary to in situ and proximal sensing measurements; ii) offer open, free and regular acquisitions.

The global and free availability of data collected by the ESA-Sentinel satellites constellations [12], which are under the umbrella of the Copernicus program, offers an unprecedented opportunity for data exploitation and for the development of new services, as a counterpart (actually complementary) to the collection of crowdsourced but inaccurate information. Differently from the former scientific missions, the Sentinel missions are offering operational services, characterised by a global coverage with guaranteed revisit times, as well as the open and free availability of the data.

This work proposes a preliminary study about using the imaging radiometer SLSTR (Sea and Land Surface Temperature Radiometer) [13, 14] onboard Sentinel-3 satellites in a non-conventional way, i.e., by exploiting its radiometric performance for estimating the water coverage within single pixels, instead of detecting and measuring the whole water surface.

SLSTRs are high accuracy radiometers selected for the Sentinel-3 (S3) component of the Copernicus services [15]. At the time of writing this paper the S3 constellation is formed by two satellites: Sentinel3A and 3B. S3A/B is the first operational satellite mission after ENVISAT that permits the simultaneous acquisition of radiometric and altimetry measurements, by hosting a radar altimeter (SRAL, Synthetic aperture Radar ALtimeter) on the same platform. Other available instruments onboard S3 are outside the scope of this manuscript, but the interested reader can find further reading in [16, 17].

978-1-7281-4460-3/20/$31.00 ©2020 IEEE

In this work, we resort to the reflectance features characterising clean water surfaces in the near- and shortwave-infrared domains (NIR and SWIR), which are typically used for water mapping [18]. Discrimination between soil and water pixels is based on the higher soil brightness with respect to water, independently from the soil coverage. Pixels including coastlines in their footprint are thus a powerful indicator of partial water coverage by precisely estimating their reflected radiation, using the sun as an illuminator.

Several single-band and multi-band indices have been proposed [19, 20] to feed binary classifiers (i.e., water/non-water) for surface water mapping. This approach requires a high spatial resolution to get meaningful results. Instead, the basic idea of this work is to use the radiance information from a single band in the NIR to estimate the partial water content within few selected pixels having coarse spatial resolution, by exploiting the precision of the radiometric measurement.

There are already some hydrological applications of this concept in the literature, in particular by using the MODIS sensor (Moderate Resolution Imaging Spectroradiometer) onboard the Terra and Aqua satellite missions by NASA. The main proposed applications regard shoreline extraction, mapping of flooded areas and river discharge estimation [21, 22].

Our experimentation with SLSTR offers the following advantages: i) nadir views have radiometric images simultaneous to altimetry measurements, permitting a cross-validation between the two techniques; ii) the short revisit time of S3A/B (half day) permits the collection of meaningful timeseries also in sites prone to frequent cloud coverage.

Finally, a novel aspect of the proposed approach is that a very limited subset of pixels takes enough information about the observed natural process, in this case a large inland water body (thousands of km^2) with varying water level.

Results of this preliminary investigation are promising in terms of good correlation between radiometric observations and altimetry measurements. Thus, there is the perspective that a very light computational process could infer an estimation of the water storage.

II. MATERIALS AND METHODS

A. Radiometric maps by SLSTR

SLSTR is a scanning radiometer, providing radiometric images in 11 channels, spanning from the visible (bands S1, S2) to the far infrared (bands S8, S9 and S8F) [14, 15].

One important feature of this instrument is the adopted conical scanning concept [23], which optimizes the radiometric calibration and the meaurement repeatability in the infrared bands, in particular thanks to the following aspects: i) the constant zenital viewing angle for all the scan points, i.e., along the whole swath; ii) the low polaristion effects, due to the constant Earth observation geometry; iii) the very frequent views of the reference blackbodies (every 0.6 s, corresponding to two successive complete rotations of the scanning system).

Figure 1 shows the swath projection onto the observed surface. The dual scan configuration (nadir and oblique views) is used to retrieve atmospheric optical parameters by using two different path lengths through the same atmospheric layer. In our experiment the acquisition is simplified to the nadir-view only.

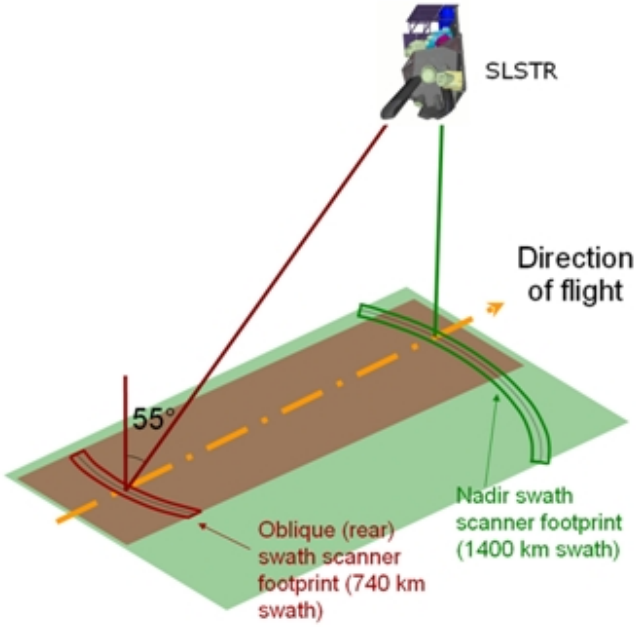

Fig. 1. Swath footprints of SLSTR instrument (picture from ESA website: https://sentinel.esa.int/web/sentinel/user-guides/sentinel-3-slstr/coverage).

The spectral channels of SLSTR are listed in Table 1. Further details about the radiometric performance of SLSTR are provided in Table 2.

Periodic calibration is performed with the aid of two blackbodies for MWIR (Middle-Wave infrared) and TIR (Thermal infrared) bands, while visible, NIR and SWIR are calibrated by a dedicated unit (VISCAL) with solar illumination input [14]. The focal plane assembly of MWIR and TIR bands is kept at cryogenic temperature (85° K), while the VIS and NIR detectors (S1 to S3) are thermally controlled at 260° K.

The radiometric images collected to build the timeseries discussed in this manuscript have been downloaded from the ESA archive through its API interface. Only Level-1 data in spectral radiance units have been used.

TABLE I. SLSTR SPECTRAL CHANNELS

Band number	Central wavelength (µm)	Bandwidth (µm)	Spatial resolution at nadir (km)
S1	0.555	0.020	0.5
S2	0.659	0.020	0.5
S3	0.870	0.020	0.5
S4	1.375	0.015	0.5
S5	1.610	0.060	0.5
S6	2.225	0.050	0.5
S7	3.700	0.380	1.0
S8	10.850	0.900	1.0
S9	12.000	1.000	1.0
S7F	3.700	0.380	1.0
S8F	12.000	0-900	1.0

TABLE II. MISCELLANEOUS CHARACTERISTICS OF SLSTR (SOURCE: ESA WEBSITE)

Channels and measurement conditions	Parameter
	Signal-to-Noise Ratio (SNR)
VIS (Albedo =0.5%)	> 20
SWIR (Albedo =0.5%)	> 20
	Noise-Equivalent Temperature difference (NEΔT)
MWIR (T =270K)	< 80 mK
TIR (T=270K)	< 50 mK
	Radiometric Accuracy
VIS-SWIR (Albedo = 2-100%)	< 2% (Beginning of Life) <5% (End of Life)
MWIR –TIR (265 – 310 K)	< 0.2 K (0.1 K goal)

B. *Altimetry profiles by SRAL*

The radar altimeter onboard S3A/B provides range measurement profiles along the orbital path. It is essentially a nadir-pointing SAR (Synthetic Aperture Radar) operating in Ku band, which provides range measurements between the antenna and the illuminated target at nadir. The revisit time of SRAL equals the full orbital cycle of S3, being the observation at nadir only, and it is equal to 27 days. S3A and S3B have interlaced orbits with constant inter-track distance (52 km at the equator) and opposite in phase. Thus, differently from SLSTR, the sampling interval between two successive altimetry measurements over the same point on earth is 27 days. The interested reader finds further information in [16].

Despite the fact that the SRAL has been designed for ocean topography applications, there is a today a mature literature demonstrating the potentiality of this class of instruments for the observation of inland water bodies [24, 25, 26].

In our study, water levels with respect to the earth reference ellipsoid have been calculated with the aid of the SARvatore processor (SAR Versatile Altimetric Toolkit for Ocean Research & Exploitation), running on the ESA GPOD (Grid Processing On Demand) service. Data are delivered at 20 Hz sampling rate, meaning that the distance between two successive measurement points on the ground is about 350 m.

C. *The study area*

The test site used for this preliminary study is the Nasser Lake, located in the southern part of the Nile River in Upper Egypt. Figure 2 shows the first available SLSTR image in the NIR band (S3 channel, central wavelength 870 nm) focusing on the study area, dated 19 June 2016. The histogram in the picture inset shows the high discriminability between the clusters of water and land pixels.

Lake Nasser is an almost ideal playground for this experiment, thanks to a series of peculiarities: i) its very limited cloud coverage; ii) the availability of multiple S3 orbits crossing the water body; iii) the complex morphological structure with variable slopes in its flanks; iv) a stable atmospheric water column (due to the dry climate) that reduces the uncertainties in the propagation of the radar signal and in the radiation transfer in the infrared domain.

Finally, the Nasser Lake is characterised by a seasonal water level variability of the order of few meters, well above the total error budget (10 cm) declared by ESA [27] for single measurements in its fully processed data (i.e. NTC, Non Time-Critical products).

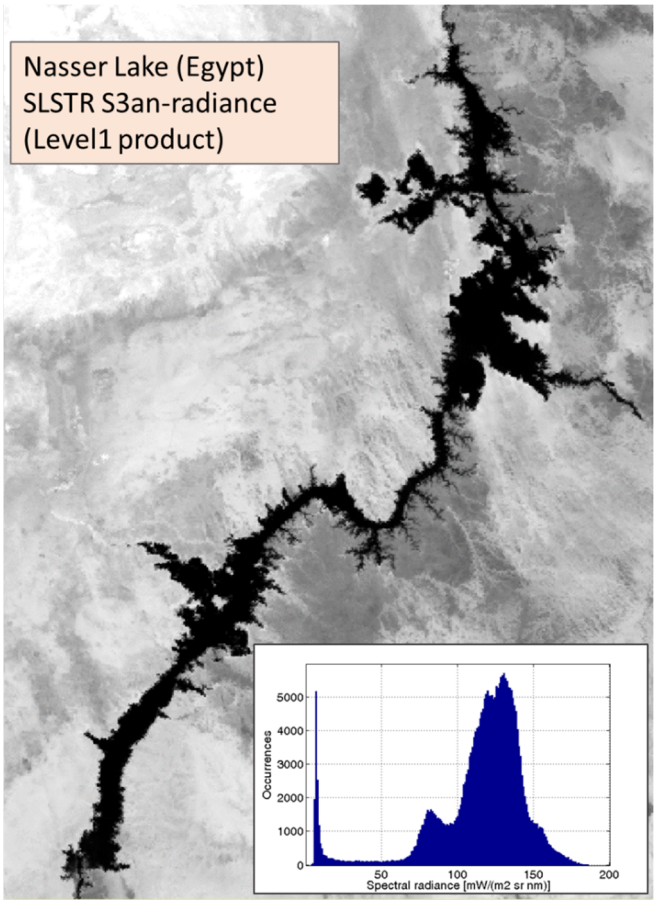

Fig. 2. Spectral radiance map in the NIR band (SLSTR S3A, nadir view). The clustering of water and non-water pixels is apparent in the histogram.

D. *Subset extraction and timeseries building*

The collected data are originated by S3A only, being the first satellite to be launched and offering > 3 years long timeseries. The relative orbit #249 is the only orbit crossing the Nasser Lake in a descending (diurnal) track, a fundamental aspect for the simultaneous acquisition by SLSTR using the sun as an illuminator. Thus, all the SRAL and SLSTR data collected by S3A in the study area, relating to orbit #249, have been downloaded from the ESA archive for this study.

The full coverage of the Nasser Lake with the native resolution of band 8 (NIR) of the MSI (Multispectral Instrument) onboard the Sentinel-2 satellite would require eight 100 km x 100 km tiles at 10 m spatial resolution. Thus, an exhaustive area calculation (necessary for estimating an area-level relationship of the water body) implies to process $800 \cdot 10^6$ pixels plus the necessary ancillary and metadata for each single band.

In our approach, co-located spatial subsets of 450x600 pixels have been extracted from each SLSTR scene and the first N pixels exhibiting the highest variability of the collected radiance are selected. To do that, a variability map is obtained by calculating the point-wise standard deviation of the measured radiance for each pixel in the whole timeseries.

As expected, the most variable pixels lie on the contour of the target, as a consequence of its morphological characteristics, and the lowest variability is found in the water body (Figure 3). All the results discussed in the next section shave been obtained with N = 100, thus, by using only 100 pixels as “sentinels” of water storage variations.

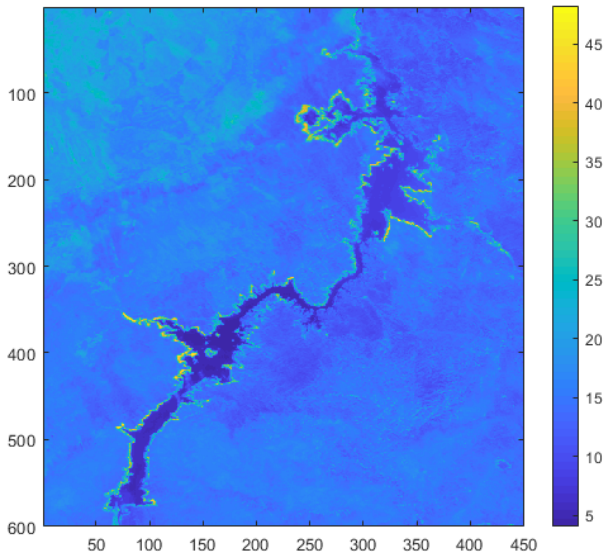

Fig. 3. Variability map (SLSTR S3A, orbit 249, nadir view). The colorscale represents the point-wise standard deviation of the spectral radiance.

III. Results

In the absence of a ground-truth dataset provided by in situ observations, the analysis of the inter-data correlation between the two independent instruments SLSTR and SRAL assumes an utmost importance. It is relevant to underline here that the availability of in situ hydrological measurements is experiencing a global reduction (mostly for budget reasons) also in developed countries, making remotely sensed measurements today even more interesting than yesterday.

We can assume the natural system as a conceptually simple single-input single-output time invariant system characterised by a non-linear transfer function, which depends on the topography of the observed site. According to this approach, the average spectral radiance of the N selected pixels can be considered as an input, and the water level measured by the satellite radar altimetry as the output parameter.

Figure 4 shows where the 100 pixels characterised by the highest variability are located, along the coastlines of the lake.

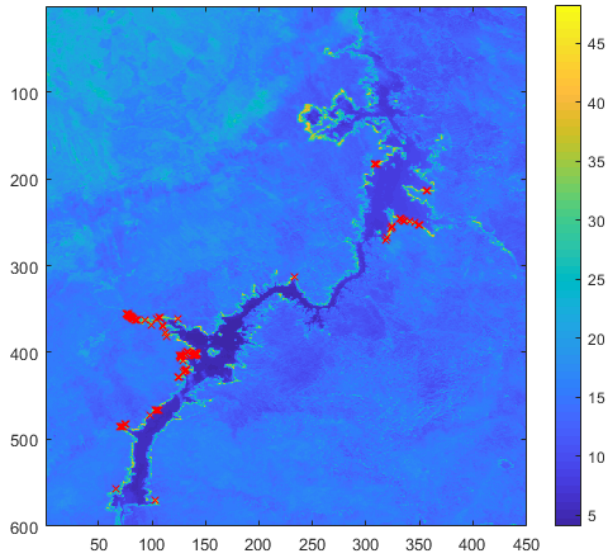

Fig. 4. Variability map (SLSTR S3A, orbit 249, nadir view). The most variable N=100 pixels are marked by red crosses.

Figures 5 and 6 show the timeseries of the averaged radiance ($-L_{avg}$) and of the water level by satellite altimetry (Orbit-Range), respectively. The sign inversion for the radiance is introduced in order to make the two plots comparable, being the water pixels the darkest ones. The (Orbit-Range) calculation provides water levels with respect to the earth reference ellipsoid.

The plotted timeseries have been built under few strong simplifying assumptions, applied to this preliminary experiment:

- the atmospheric path delays and extinction are considered constant, thus no atmospheric correction is applied;

- no estimation of water coverage percent within contouring pixels is done. Spectral radiances of the most variable ones are just averaged per each satellite pass;

- the lake is considered hydraulically static, i.e., the selected points for water level assessment by altimetry are considered as representative of the water level of the whole lake.

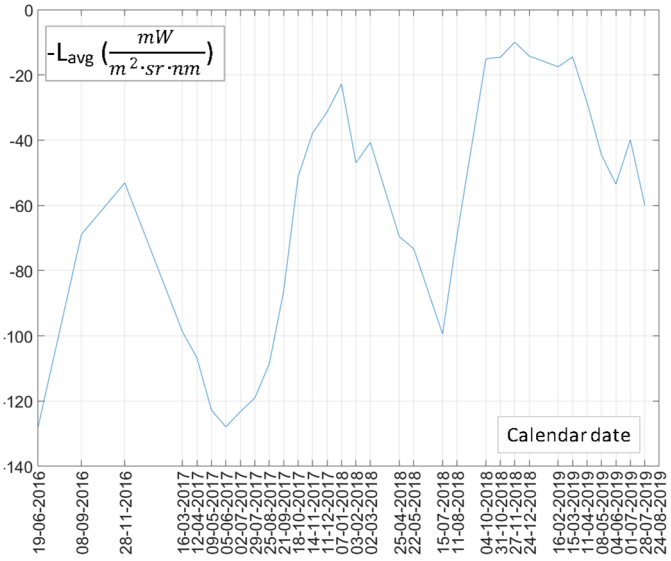

Fig. 5. Timeseries of averaged spectral radiance over the selected N=100 points (SLSTR S3A, orbit 249, nadir view).

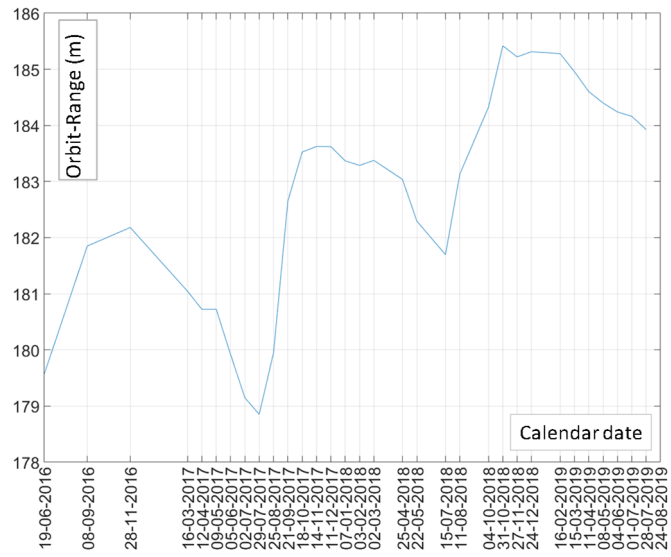

Fig. 6. Timeseries of water level by satellite radar altimetry (SRAL S3A, orbit 249).

Interestingly, the two plots share a similar inter-annual trend and exhibit a comparable seasonal behaviour.

The measurement points for water level estimations by satellite altimetry lie along the red line plotted on the lake contour shown in Figure 7.

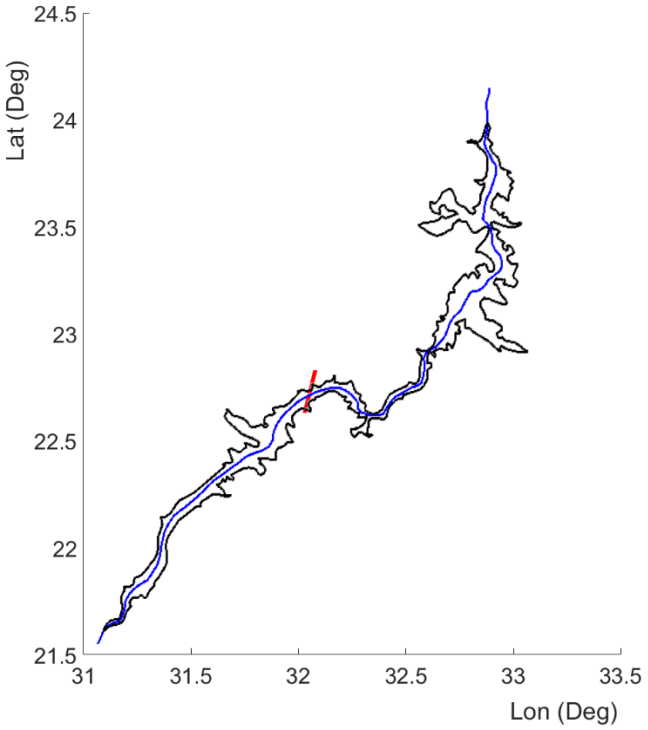

Fig. 7. Lake contour line (black), center line (blue) and segment of the satellite orbit used for altimetry measurements (red).

Finally, Figure 8 shows the scatterplot and a 2nd-order polynomial approximation to the I/O relationship between the two analysed parameters. The 2nd-order polynomial was chosen in order to guarantee monotonicity. The obtained R^2 is 0.89.

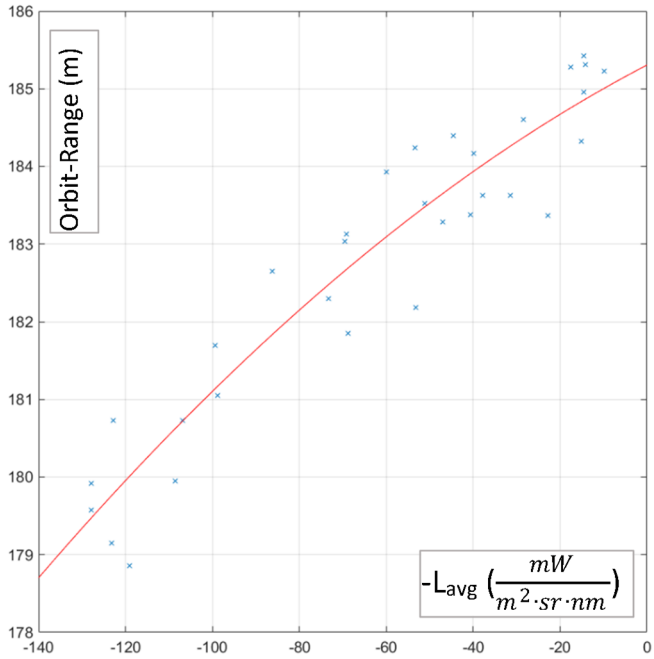

Fig. 8. Scatterplot of the simultaneous radiometric and altimetry measurements in all the timeseries analysed. The 2nd-order polynomial fitting function is plotted in red.

IV. Conclusions

The usage of radiometric measurements for quantifying hydrological parameters has multiple advantages, such as: i) the possibility to monitor targets not crossed by the satellite altimeters' tracks; ii) the possibility to monitor completely ungauged sites; iii) the availability of a complementary and independent measurement in addition to altimetry, when altimetry is available.

Under the hypothesis of a time-invariant system (i.e., no significant morphological changes), once an area-level-volume relationship is identified, volume estimations can be inferred by either altimetry (i.e., level) or radiometric measurements per se. Thus, the simultaneous measurements by the two instruments constitutes an excellent opportunity for: i) cross-validating the acquired data; ii) making expedite estimations of volume variations.

Finally, by using the approximation proposed in this paper, a very light computational process can infer an estimation of water storage, when the natural system is fully identified on the basis of ground-truth data.

Acknowledgment

The authors acknowledge the financial support from the Academy of Scientific Research and Technology (ASRT) of Egypt and the Italian National Research Council (CNR) via the bilateral CNR-ASRT project titled "Experimentation of the new Sentinel missions for the observation of inland water bodies on the course of the Nile River".

References

[1] A. Bustanul, P. Irwan and M. T. Andi, "The development and design of LAPAN's IR camera equipped with micro bolometer sensor," 2017 IEEE International Geoscience and Remote Sensing Symposium (IGARSS), Fort Worth, USA, 2017, pp. 530-533, doi: 10.1109/IGARSS.2017.8127007J.

[2] A. M. Jensen, M. McKee and Y. Chen, "Procedures for processing thermal images using low-cost microbolometer cameras for small unmanned aerial systems," 2014 IEEE Geoscience and Remote Sensing Symposium, Quebec City, QC, 2014, pp. 2629-2632, doi: 10.1109/IGARSS.2014.6947013.

[3] R. Battaglini, B. Raco, and A. Scozzari. "Effective monitoring of landfills: flux measurements and thermography enhance efficiency and reduce environmental impact." Journal of Geophysics and Engineering 10.6 (2013): 064002.

[4] T. Arnold, M. De Biasio, A. Fritz and R. Leitner, "UAV-based measurement of vegetation indices for environmental monitoring," 2013 IEEE International Conference on Sensing Technology (ICST), Wellington, 2013, pp. 704-707, doi: 10.1109/ICSensT.2013.6727744

[5] B. Han and T. A. Endreny, "River Surface Water Topography Mapping at Sub-Millimeter Resolution and Precision With Close Range Photogrammetry: Laboratory Scale Application," in IEEE Journal of Selected Topics in Applied Earth Observations and Remote Sensing, vol. 7, no. 2, pp. 602-608, Feb. 2014, doi: 10.1109/JSTARS.2014.2298452

[6] Z. Zhang, T. Zhang, J. Zhou, Y. Lu and Y. Qiao, "Mobile phone Camera Based Visible Light Communication Using Non-Line-of-Sight (NLOS) Link," 2018 IEEE International Conference on Network Infrastructure and Digital Content (IC-NIDC), Guiyang, 2018, pp. 35-39, doi: 10.1109/ICNIDC.2018.8525559.

[7] R. Copperwhite, C. McDonagh and S. O'Driscoll, "A Camera Phone-Based UV-Dosimeter for Monitoring the Solar Disinfection (SODIS) of Water," in IEEE Sensors Journal, vol. 12, no. 5, pp. 1425-1426, May 2012, doi: 10.1109/JSEN.2011.2172938.

[8] M. Santonico, A. Scozzari, G. Brozzo, L. Marini, A. D'Amico, D. Filippini, .I. Lundström, C. Di Natale, "Detection of natural Cr (VI) with computer screen photo-assisted technology." Procedia Chemistry 1.1 (2009): 317-320, doi: 10.1016/j.proche.2009.07.079.

[9] S. Ozehl, A. G. Nnanna, and J. C. Ndukaife. "Smartphone-Based Device for Monitoring Chemical Pollutants in Water." ASME 2018 International Mechanical Engineering Congress and Exposition. American Society of Mechanical Engineers Digital Collection, 2018.

[10] M. Mazzoleni., L. Alfonso, D. P. Solomatine (2019) "Exploring Assimilation of Crowdsourcing Observations into Flood Models". In: . D. Han, S. Mounce, A. Scozzari, F. Soldovieri, and D. Solomatine (eds.), "ICT for Smart Water Systems: Measurements and Data Science", The Handbook of Environmental Chemistry. Springer, Berlin, Heidelberg.

[11] A. M. de Oca, L. Arreola, A. Flores, J. Sanchez and G. Flores, "Low-cost multispectral imaging system for crop monitoring," 2018 International Conference on Unmanned Aircraft Systems (ICUAS), Dallas, TX, 2018, pp. 443-451, doi: 10.1109/ICUAS.2018.8453426.

[12] European Space Agency, "Missions - Sentinel Online.", sentinel.esa.int/web/sentinel/missions (date accessed: 24 Nov. 2019)

[13] P. Coppo, C. Mastrandrea, M. Stagi, L. Calamai, J. Nieke, "Sea and Land Surface Temperature Radiometer detection assembly design and performance." Journal of Applied Remote Sensing 8.1 (2014): 084979.

[14] D. L. Smith et al. "Calibration approach and plan for the sea and land surface temperature radiometer." Journal of Applied Remote Sensing 8.1 (2014): 084980.

[15] P. Coppo et al., "The sea & land surface temperature radiometer (SLSTR) technologies", 61st International Astronautical Congress 2010, International Astronautical Federation.

[16] C. Donlon, "The global monitoring for environment, and security (GMES) Sentinel 3 mission", Remote Sens. Environ. 120, 37–57 (2012).

[17] European Space Agency, "Sentinel3 - Instrument Payload - Sentinel Online.", sentinel.esa.int/web/sentinel/missions/sentinel-3/instrument-payload (date accessed: 24 Nov. 2019)

[18] R. Malinowski, G. Groom, W. Schwanghart, H. Goswin, "Detection and Delineation of Localized Flooding from WorldView-2 Multispectral Data", Remote Sensing, 7 (2015) 14853-14875, doi:10.3390/rs71114853.

[19] Y. Zhou et al. "Open surface water mapping algorithms: A comparison of water-related spectral indices and sensors." Water 9.4 (2017): 256.

[20] M. Jollineau and P. Howarth, "Use of high-resolution imagery to map wetland environments in south-central Ontario, Canada," IEEE International Geoscience and Remote Sensing Symposium, Toronto, Ontario, Canada, 2002, pp. 3089-3091 vol.5. doi: 10.1109/IGARSS.2002.1026878

[21] G. Ovakoglou, T. K. Alexandridis, T. L. Crisman, C. Skoulikaris, G. S. Vergos, "Use of MODIS satellite images for detailed lake morphometry: Application to basins with large water level fluctuations", International Journal of Applied Earth Observation and Geoinformation, vol. 51, pp. 37-46, 2016, doi: 10.1016/j.jag.2016.04.007.

[22] A. Tarpanelli, L. Brocca, T. Lacava, F. Melone, T. Moramarco, M. Faruolo, N. Pergola, V. Tramutoli, "Toward the estimation of river discharge variations using MODIS data in ungauged basins", Remote Sensing of Environment, vol. 136, 2013, pp. 47-55, doi: 10.1016/j.rse.2013.04.010.

[23] Coppo, P., B. Ricciarelli, F. Brandani, J. Delderfield, M. Ferlet, C. Mutlow, G. Munro, T. Nightingale, D. Smith, S. Bianchi, P. Nicol, S. Kirschstein, T. Hennig, W. Engel, J. Frerick & J. Nieke, "SLSTR: a high accuracy dual scan temperature radiometer for sea and land surface monitoring from space," J. Mod. Opt. 57(18), 1815–1830, 2010

[24] C. Schwatke, D. Dettmering, W. Bosch, and F. Seitz, "DAHITI–an innovative approach for estimating water level time series over inland waters using multi-mission satellite altimetry." Hydrology and Earth System Sciences 19.10 (2015): 4345-4364.

[25] Crétaux, J-F., et al. "SOLS: A lake database to monitor in the Near Real Time water level and storage variations from remote sensing data." Advances in space research 47.9 (2011): 1497-1507.

[26] S. Vignudelli, A. Scozzari, R. Abileah, J. Gomez-Enri, P.Cipollini, J. Benveniste, "Water surface elevation in coastal and inland waters using satellite radar altimetry." Extreme Hydroclimatic Events and Multivariate Hazards in a Changing Environment: A Remote Sensing Approach (2019): 87.

[27] European Space Agency, "Sentinel3 - ESA's Global Land and Ocean Mission for GMES Operational Services", ESA document SP-1322/3, October 2012